Joint Maximum Likelihood Estimation for Time and Frequency Synchronization

Yingming Tsai and Guodong Zhang
InterDigital Communications Corporation
2 Huntington Quadrangle
Melville, NY 11747, USA
Yingming.Tsai@, Guodong.Zhang@interdigital.com

Xiaodong Wang
ECE Dept., Columbia University
2960 Broadway
New York, New York 10027
xwang@ece.columbia.edu

Abstract— A new repetitive synchronization signal structure is proposed for wireless communication systems. A corresponding joint maximum likelihood detection algorithm that uses the proposed synchronization signals is provided. The joint maximum likelihood detection algorithm combines the advantages of non-coherent and coherent maximum likelihood detection algorithms. The performance of our approach is evaluated and compared to other existing algorithms.

Keywords: Synchronization, Joint maximum likelihood estimation

I. INTRODUCTION

In order for a wireless communications system to receive downlink data properly, the mobile terminal first needs to acquire the downlink timing and carrier frequency offset. The acquisition of downlink timing and frequency offset is usually called synchronization or cell search.

In the past few years, extensive research has been done on time and frequency synchronization in wireless communication systems [1-9]. Synchronization signals with repetition blocks in the time domain have been used with auto-correlation based timing and frequency detection algorithms [3-8]. Synchronization signals with a non-repetitive pattern and a cross-correlation based detection algorithm have also been proposed in [1-2]. These signal structures and their corresponding detection algorithms all have their design limitations and performance trade-offs. In this paper, we propose a new method to generate synchronization signals with a repetitive pattern to overcome the design limitations of these methods. We also apply a joint maximum likelihood (ML) detection algorithm to acquire timing and frequency offset.

The rest of the paper is organized as follows. In Section II, the system model of synchronization is described and formulated. In Section III, a new synchronization signal structure is proposed. A corresponding joint maximum likelihood detection algorithm that uses the proposed synchronization signals is described. The numerical results are obtained and discussed in Section IV. Finally, conclusions are drawn in Section V.

II. SYSTEM MODEL

In this section, we consider the generic synchronization (sync) signal structure. First, we define the following notations: $(\ )^T$ stands for transport operation, $(\ )^H$ stands for Hermitian operation, $\otimes$ stands for matrix Kronecker product, and T^{μ} stands for shift operator with a shift of μ. Without loss of generality, we assume that the transmitted data consists of a data sequence of length *P* followed by a sync signal of length *K*, as shown in Figure 1. Let N denote the frame length. The transmitted frame signal vector $\mathbf{x} = [\mathbf{s}^T \,|\, \mathbf{d}_{N-K}{}^T]^T$, where $\mathbf{s} = [s_0, \ldots, s_{K-1}]^T$ is the sync signal and $\mathbf{d}_{N-K}$ = $[d_K, \ldots, d_{N-1}]^T$ is the transmitted data symbol vector with a length of $N-K$. In practice, sync signals are usually limited to those with symmetric signal constellations and unit energy, i.e., only those that use M-PSK constellations. Let μ denote the downlink timing. Let θ denote the normalized carrier frequency offset with a uniform distribution between $[-\theta_m, \ldots, \theta_m]$, where θ_m is the maximum normalized frequency offset.

The observed received signal vector of length N, denoted as $\mathbf{y}$, is expressed as

$$\mathbf{y} = \varphi_D T^{\mu} \mathbf{x} + \mathbf{w}, \qquad (1)$$

where $\boldsymbol{\varphi}_D = diag\{e^{j2\pi k\theta}, \ldots, e^{j2\pi(k+N-1)\theta}\}$ is a vector of size N and w is AWGN with variance N_0. In the synchronization process, the mobile terminal detects timing μ and frequency offset θ from the *N* received samples $\{y_0, y_1, \ldots, y_{N-1}\}$.

III. COHERENT ML ESTIMATOR

Suppose that the received sync signal starts at the µth sample of received *N* samples, as shown in Figure 1. Then, the conditional probability density function (pdf) of received signal $\mathbf{y}$, given μ, θ and $\mathbf{d}_{N-K}$, can be expressed as

$$p(\mathbf{y}|\mu,\theta,\mathbf{d}_{N-K}) = \frac{e^{-(\mathbf{y}-\sqrt{E_s}\,\boldsymbol{\varphi}_D T^{\mu}\mathbf{x})^H R_w^{-1}(\mathbf{y}-\sqrt{E_s}\,\boldsymbol{\varphi}_D T^{\mu}\mathbf{x})}}{\pi^N \det(R_w)}$$
$$= \frac{e^{-E_s/N_o\left\|\mathbf{y}-\boldsymbol{\varphi}_D T^{\mu}\mathbf{x}\right\|^2}}{\pi^N N_o^N}, \quad (2)$$

where $R_w = E\{\mathbf{w}^H\mathbf{w}\}$ is the autocorrelation matrix of $\mathbf{w}$. The coherent maximum likelihood estimate of μ and θ is equivalent to the maximization of the conditional pdf of received signal $\mathbf{y}$, i.e., $p(\mathbf{y}|\mu,\theta,\mathbf{d}_{N-K})$, with respect to μ, θ and $\mathbf{d}_{N-K}$.

After taking the logarithm on both sides of (2) and dropping terms independent of μ and θ, the log likelihood function is written as

$$L(\mu,\theta,\mathbf{d}_{N-K}) = \frac{2\sqrt{E_s}}{N_o}\mathrm{Re}\{(\boldsymbol{\varphi}_D T^{\mu}\mathbf{x})^H\mathbf{y}\} = \frac{2\sqrt{E_s}}{N_o}\mathrm{Re}\{(\boldsymbol{\varphi}_D\mathbf{x})^H T^{\mu}\mathbf{y}\}$$
$$= \frac{2\sqrt{E_s}}{N_o}\mathrm{Re}\{(\boldsymbol{\varphi}_{D,K}\mathbf{s})^H T^{\mu}\mathbf{y}_K\} +$$
$$\frac{2\sqrt{E_s}}{N_o}\mathrm{Re}\{(\boldsymbol{\varphi}_{D,N-K}\mathbf{d}_{N-K})^H T^{\mu}\mathbf{y}_{N-K}\}, \quad (3)$$

where we have $\mathbf{y}_K = \{y_0,\ldots,y_{K-1}\}$, $\mathbf{y}_{N-K} = \{y_K,\ldots,y_{N-1}\}$, $\boldsymbol{\varphi}_{D,K} = diag\{e^{j2\pi k\theta},\ldots,e^{j2\pi(k+K-1)\theta}\}$, and $\boldsymbol{\varphi}_{D,N-K} = diag\{e^{j2\pi(k+K)\theta},\ldots,e^{j2\pi(k+N-1)\theta}\}$.

We assume that transmitted data d_k is uniformly distributed. After averaging the second term of (3) over all possible data sequences, the function can be rewritten as

$$\mathrm{Re}\{(\boldsymbol{\varphi}_{D,N-K}\mathbf{d}_{N-K})^H T^{\mu}\mathbf{y}_{N-K}\} = \mathrm{Re}\{(\boldsymbol{\varphi}_D\mathbf{d})^H T^{\mu}\mathbf{y}\} - \mathrm{Re}\{(\boldsymbol{\varphi}_{D,K}\mathbf{d}_K)^H T^{\mu}\mathbf{y}_K\}, \quad (4)$$

where $\boldsymbol{\varphi}_K = \{e^{j\pi k\theta},\ldots,e^{j\pi(K-1)\theta}\}$. Applying (4) to (3), and dropping the term $\mathrm{Re}\{(\boldsymbol{\varphi}_D\mathbf{d}_N)^H T^{\mu}\mathbf{y}\}$ because it is independent of μ and θ for any transmitted data sequence $\mathbf{d}$, the coherent ML estimate of μ and θ in (3) is equivalent to the maximization of the likelihood function below:

$$\Lambda^C(\mu,\theta) = \arg\max_{\mu,\theta}\mathrm{Re}\{(\boldsymbol{\varphi}_{D,K}\mathbf{s})^H\mathbf{z}_K\} - \mathrm{Re}\{(\boldsymbol{\varphi}_{D,K}\mathbf{d}_K)^H\mathbf{z}_K\}, \quad (5)$$

where $\mathbf{z}_K$ denotes the subvector $\{z_0,\ldots z_{K-1}\}$ of observed received signals $\mathbf{z} = T^{\mu}\mathbf{y}$. Note that when frequency offset θ is not present, (5) becomes the same as the coherent ML estimator in [1-2].

In order to acquire the time and frequency offset using the ML estimator in (5), μ and θ have to be estimated jointly. This can be achieved by using an algorithm with extensive complexity such as the EM algorithm [9]. Alternatively, a non-coherent ML estimator [2] can be used to avoid the joint estimation of μ and θ; this reduces the estimation parameter to one, e.g., timing μ. However, each of these algorithms has its own inherent trade-off in terms of complexity and performance. They are either unable to achieve the optimal performance or they suffer performance degradation under low SNR. This motivates us to design a more efficient approach.

IV. Proposed Sync Signal Structure and Joint ML Estimator

In this paper, we propose an alternative to the joint estimation approach. The proposed estimation algorithm relies on the particular sync signal structure we first proposed in [11] for an OFDMA based system and further extend in this paper for any generic wireless communications system.

A. *Proposed sync signal structure*

It is known that a synchronization signal with 2 repetitions [3] results in a plateau in the timing detection metric, which causes poor timing localization. It was shown in [4] that a larger number of repetitions (>2) can mitigate the problem, and a theoretical performance analysis was provided in [5].

To address this issue (plateau in detection metric), we propose a method to generate repetition blocks in the time domain different from the one proposed in [3-5]. A new sync signal structure $\mathbf{s} = [A_{K/4}\ -B_{K/4}\ A_{K/4}\ B_{K/4}]$ where sequences A and B meet the condition that $E\{A^H B\} = 0$ was proposed in [11], as shown in Figure 2. One of special cases is to let $B(k) = A(\frac{K}{4}-k)$, i.e., to let sequence B be symmetrical to sequence A [6]. The key advantage of the proposed method is that it not only eliminates the plateau in the timing detection metric but also provides a sharper peak than the sync signal $[A_{K/4}\ -A_{K/4}\ A_{K/4}\ A_{K/4}]$ defined in [4].

B. *Proposed joint ML estimator*

The joint ML estimation consists of two steps: a non-coherent ML estimator is used first, and a coherent ML estimator is used second. To reduce the two-dimensional estimation into one-dimensional estimation (timing offset only), the frequency offset θ is estimated in the first step before the coherent ML estimator is used in the second step.

Step 1: The conditional probability density function of received signal is given by

$$p(\mathbf{z}|\mu,\theta) = \frac{1}{\pi^K \det(R_{\mathbf{z}})^{-1}} e^{-\mathbf{z}^H R_{\mathbf{z}}^{-1}\mathbf{z}}, \quad (6)$$

which yields the non-coherent log-likelihood function, given as

$$L^{NC}(\mu,\theta) = -\ln(\pi^K) - \ln\det R_{\mathbf{z}}^{-1} - \mathbf{z}^H R_{\mathbf{z}}^{-1}\mathbf{z}\ . \quad (7)$$

The maximization of the non-coherent log-likelihood function in (7) is equivalent to the minimization of the following cost function

$$\Lambda^{NC}(\mu,\theta)=\arg\min_{\mu,\theta} -\mathbf{z}^H R_{\mathbf{z}}^{-1}\mathbf{z}, \quad (8)$$

where $R_{\mathbf{z}} = \boldsymbol{\varphi}_D R_{\mathbf{x}} \boldsymbol{\varphi}_D^H + I$. As we further analyze $\ln\det R_{\mathbf{z}}^{-1} = \ln\det(\boldsymbol{\varphi}_D)\det(R_{\mathbf{x}} + N_o\mathbf{I})^{-1}\det(\boldsymbol{\varphi}_D)^H = \ln\det(R_{\mathbf{x}} + N_o\mathbf{I})^{-1}$, it becomes obvious that it is independent of μ, θ. Therefore, the term $\ln\det R_{\mathbf{z}}^{-1}$ is dropped in (8). Furthermore, by using linear algebra, the $\Lambda^{NC}(\mu,\theta)$ can be rewritten as

$$\Lambda^{NC}(\mu,\theta)=\arg\min_{\mu,\theta} -\mathbf{z}^H R_{\mathbf{z}}^{-1}\mathbf{z}$$
$$=\arg\min_{\mu,\theta} -\mathbf{z}^H\left(\boldsymbol{\varphi}_D R_{\mathbf{x}}\boldsymbol{\varphi}_D^H + N_o\mathbf{I}\right)^{-1}\mathbf{z}. \quad (9)$$

To solve $\Lambda^{NC}(\mu,\theta)$, we need to examine the inverse matrix of $R_{\mathbf{z}} = \boldsymbol{\varphi}_D R_{\mathbf{x}}\boldsymbol{\varphi}_D^H + N_o\mathbf{I}$. If $R_{\mathbf{x}} = \mathbf{I}$ (i.e., no sync signal structure is used), then $R_{\mathbf{z}} = E_s\boldsymbol{\varphi}_D\boldsymbol{\varphi}_D^H + N_o\mathbf{I} = (E_s + N_o)\mathbf{I}$. Hence, no prior information can be obtained from the non-coherent estimator without using a sync signal structure. The autocorrelation function of the proposed sync signal is given by

$$\zeta_z(m) = E\{z(k)z^*(k+m)\}$$
$$=\begin{cases} E_s + N_o, & m=0, \quad \forall k \\ E_s e^{-j\pi K\theta}, & m=\frac{K}{2}, \quad 0\le k\le \frac{K}{4}-1 \\ -E_s e^{-j\pi K\theta}, & m=\frac{K}{2}, \quad \frac{K}{4}\le k\le\frac{K}{2}-1 \\ 0, & \text{otherwise} \end{cases}. \quad (10)$$

Based on (10), the autocorrelation of $R_{\mathbf{z}}$ can be expressed as

$$R_{\mathbf{z}} = \begin{bmatrix} \boldsymbol{\Psi}_K & 0 \\ 0 & \boldsymbol{\Psi}_{N-K} \end{bmatrix}, \quad (11)$$

where $\boldsymbol{\Psi}_{N-K} = (E_s + N_o)I_{N-K}$, $\rho = \frac{SNR}{1+SNR}$, and $\boldsymbol{\Psi}_K$ is given by

$$\boldsymbol{\Psi}_K = (E_s + N_o)\underbrace{\begin{bmatrix} 1 & 0 & \rho e^{-j\pi K\theta} & 0 \\ 0 & 1 & 0 & -\rho e^{-j\pi K\theta} \\ \rho e^{j\pi K\theta} & 0 & 1 & 0 \\ 0 & -\rho e^{j\pi K\theta} & 0 & 1 \end{bmatrix}}_{\mathrm{X}} \otimes I_{K/4}. \quad (12)$$

We know that the inverse matrix of R_z is equal to $diag\left[\boldsymbol{\Psi}_K^{-1}, \boldsymbol{\Psi}_{N-K}^{-1}\right]$. Therefore, $\boldsymbol{\Psi}_K^{-1}$ can be expressed as

$$\boldsymbol{\Psi}_K^{-1} = (E_s + N_o)\mathrm{X}^{-1}\otimes I_{K/4}^{-1}$$
$$=\frac{E_s + N_o}{1-\sigma^2}\underbrace{\begin{bmatrix} 1 & 0 & -\rho e^{-j\pi K\theta} & 0 \\ 0 & 1 & 0 & \rho e^{-j\pi K\theta} \\ -\rho e^{j\pi K\theta} & 0 & 1 & 0 \\ 0 & \rho e^{j\pi K\theta} & 0 & 1 \end{bmatrix}}_{\mathrm{X}} \otimes I_{K/4}. \quad (13)$$

Using (11-13), (9) can be rewritten as

$$\Lambda^{NC}(\mu,\theta) = \arg\min_{\mu,\theta} -\mathbf{z}^H R_{\mathbf{z}}^{-1}\mathbf{z} = \arg\min_{\mu,\theta} -[\mathbf{z}_K^H, \mathbf{z}_{N-K}^H]R_{\mathbf{z}}^{-1}[\mathbf{z}_K, \mathbf{z}_{N-K}]$$
$$= \arg\min_{\mu,\theta} -(E_s + N_o)\left[\frac{1}{1-\rho^2}\mathbf{z}_K^H\boldsymbol{\Psi}_K^{-1}\mathbf{z}_K + \mathbf{z}_{N-K}^H\mathbf{z}_{N-K}\right]$$
$$= \arg\min_{\mu,\theta} -(E_s + N_o)\left[\frac{1}{1-\rho^2}\mathbf{z}_K^H\boldsymbol{\Psi}_K^{-1}\mathbf{z}_K + \mathbf{z}^H\mathbf{z} - \mathbf{z}_K^H\mathbf{z}_K\right]$$
$$= \arg\min_{\mu,\theta} -\frac{E_s + N_o}{1-\rho^2}\left[\mathbf{z}_K^H\boldsymbol{\Psi}_K^{-1}\mathbf{z}_K - (1-\rho^2)\mathbf{z}_K^H\mathbf{z}_K\right]. \quad (14)$$

The term $\mathbf{z}^H\mathbf{z}$ is dropped in (14) because it is independent of μ and θ. To estimate μ and θ, the non-coherent likelihood function is applied over a window of length K instead of length N. Let β denote $(E_s + N_o)/(1-\rho^2)$. Using (13), (14) can be further simplified as

$$\Lambda^{NC}(\mu,\theta) = \arg\min_{\mu,\theta} -\beta\left[\mathbf{z}_K^H\boldsymbol{\Psi}_K^{-1}\mathbf{z}_K - (1-\rho^2)\mathbf{z}_K^H\mathbf{z}_K\right]$$
$$= \arg\min_{\mu,\theta} -\rho\beta\left[\rho\ \mathbf{z}_K^H\mathbf{z}_K\right.$$
$$\left. + 2\,\mathrm{Re}\left\{e^{-j\pi K\theta}(\mathbf{z}_{1,K/4}^H\mathbf{z}_{3,K/4} - \mathbf{z}_{2,K/4}^H\mathbf{z}_{4,K/4})\right\}\right], \quad (15)$$

where $z_{m,K/4} = \{z(k)\}$ and $(m-1)\frac{K}{4}\le k\le m\frac{K}{4}-1$. Hence, using the non-coherent ML estimator, the timing offset is estimated as

$$\hat{\mu}^{NC} = \mathrm{Re}\left\{e^{-j\pi K\theta}(\mathbf{z}_{1,K/4}^H\mathbf{z}_{3,K/4} - \mathbf{z}_{2,K/4}^H\mathbf{z}_{4,K/4})\right\} - \frac{\rho}{2}\mathbf{z}_K^H\mathbf{z}_K. \quad (16)$$

In the case of high SNR, we have $\rho\to 1$. Then, $\hat{\mu}^{NC}$ can be approximated as

$$\hat{\mu}^{NC} = \left|\mathbf{z}_{1,K/4}^H\mathbf{z}_{3,K/4} - \mathbf{z}_{2,K/4}^H\mathbf{z}_{4,K/4}\right|. \quad (17)$$

Therefore, the estimation of $\hat{\mu}^{NC}$ in the case of high SNR does not require the SNR estimation. Instead, the estimation of $\hat{\mu}^{NC}$ is based on the auto-correlation of received signals, as in (17). However, the timing offset estimator $\hat{\mu}^{NC}$ is not optimal. An alternative timing offset estimator is expressed as

$$\hat{\mu}_{Proposed} = \left|-\mathbf{z}_{1,K/4}^H\tilde{\mathbf{z}}_{2,K/4} - \tilde{\mathbf{z}}_{2,K/4}^H\mathbf{z}_{3,K/4} + \mathbf{z}_{3,K/4}^H\tilde{\mathbf{z}}_{4,K/4}\right| + +\left|\mathbf{z}_{1,K/4}^H\tilde{\mathbf{z}}_{4,K/4}\right|$$
$$+\left|-\mathbf{z}_{2,K/4}^H\mathbf{z}_{4,K/4} + \mathbf{z}_{1,K/4}^H\mathbf{z}_{3,K/4}\right| - \frac{3\sigma}{2}\mathbf{z}_K^H\mathbf{z}_K, \quad (18)$$

where $\tilde{\mathbf{z}}_{m,K/4}$ stands for the symmetrical vector of $z_{m,K/4}$, i.e., $\tilde{z}(k) = z(\frac{K}{4}-k)$. In the meantime, using the non-coherent ML estimator, the frequency offset is estimated as

$$\hat{\theta}^{NC} = \frac{1}{\pi K}\arg(\mathbf{z}_{1,K/4}^H\mathbf{z}_{3,K/4} - \mathbf{z}_{2,K/4}^H\mathbf{z}_{4,K/4}), \quad (19)$$

where $\arg\{x\}$ is the phase of a complex number x.

Step 2: In this step, the value of the frequency offset $\hat{\theta}^{NC}$ obtained in step 1 is plugged into the coherent ML estimator in (5). Therefore, using the coherent ML estimator, the timing offset is estimated as

$$\mu^C = \mathrm{Re}\left\{(\hat{\boldsymbol{\varphi}}_{D,K}\mathbf{s})^H \mathbf{z}_K\right\} - \mathrm{Re}\left\{(\hat{\boldsymbol{\varphi}}_{D,K}\mathbf{d}_K)^H \mathbf{z}_K\right\}, \qquad (20)$$

where $\hat{\boldsymbol{\varphi}}_{D,K} = diag\{e^{j2\pi\hat{\theta}}, \ldots, e^{j2\pi K\hat{\theta}}\}$ is the diagonal matrix of the estimated phase $\hat{\theta}^{NC}$.

In a special case where $\mathbf{d}_K$ is QPSK modulated, (20) can be expressed as

$$\mu^C = \mathrm{Re}\left\{(\hat{\boldsymbol{\varphi}}_{D,K}\mathbf{s})^H \mathbf{z}_K\right\} - \mathrm{Re}\{\mathbf{z}_K\} . \qquad (21)$$

In this case, (21) can be interpreted as the cross-correlation based estimator proposed in [1-2].

V. Performance Analysis and Numerical Results

In this section, we evaluate several estimators using corresponding sync signal structures proposed by [3-6]. The timing and frequency offset, based on the sync signal structure with two repetitions proposed by Schmidt [3], are expressed as

$$\hat{\mu}_{\mathrm{Schmidt}} = \left|\mathbf{z}_{1,K/2}^H \mathbf{z}_{2,K/2}\right| , \qquad (22)$$

$$\hat{\theta}_{\mathrm{Schmidt}} = \frac{1}{\pi K} \arg(\mathbf{z}_{1,K/2}^H \mathbf{z}_{2,K/2}) . \qquad (23)$$

The timing and frequency offset, based on the sync signal structure with four repetitions proposed by Minn [4] and Shi [5], are given by

$$\hat{\mu}_{Minn} = \left| -\mathbf{z}_{1,K/4}^H \mathbf{z}_{2,K/4} - \mathbf{z}_{2,K/4}^H \mathbf{z}_{3,K/4} + \mathbf{z}_{3,K/4}^H \mathbf{z}_{4,K/4} \right| \qquad (24)$$

$$\hat{\mu}_{Shi} = \left| -\mathbf{z}_{1,K/4}^H \mathbf{z}_{2,K/4} - \mathbf{z}_{2,K/4}^H \mathbf{z}_{3,K/4} + \mathbf{z}_{3,K/4}^H \mathbf{z}_{4,K/4} \right| + \left| -\mathbf{z}_{2,K/4}^H \mathbf{z}_{4,K/4} + \mathbf{z}_{1,K/4}^H \mathbf{z}_{3,K/4} \right| + \left| \mathbf{z}_{1,K/4}^H \mathbf{z}_{4,K/4} \right| , \qquad (25)$$

$$\hat{\theta}_{Shi} = \frac{2}{\pi K} \arg(-\mathbf{z}_{1,K/4}^H \mathbf{z}_{2,K/4} - \mathbf{z}_{2,K/4}^H \mathbf{z}_{3,K/4} + \mathbf{z}_{3,K/4}^H \mathbf{z}_{4,K/4}) . \qquad (26)$$

The performance of the timing and frequency detection algorithms using corresponding sync signals structures were simulated and compared. Simulation parameters are summarized in Table 1. A Frank sequence [10] is used as the basic sequence to build the sync signals. We assume that the accumulation length for timing and frequency offset acquisition is one radio frame (10 msec) [12].

TABLE I. Synchronization Channel Simulation Parameters

Transmission BW	1.25 MHz
Carrier frequency	2 GHz
FFT Size	128
Data symbol length	384
Length of synchronization sequence	64
Number of sync symbols per 10 msec frame	4
Carrier frequency offset	+/- 3 ppm
Channel Model	AGWN

For the purposes of fair comparison, the same Ep/N0 is assumed for all the methods (different sync symbol structures). Timing and frequency offset detection are considered to be successful if the acquired timing falls within the duration of +/-1 sample and frequency offset is corrected.

The miss detection probabilities of the non-coherent ML estimation algorithms using existing and proposed sync signal structures are plotted in Figure 3. Among non-coherent ML estimation algorithms, the algorithm using our proposed sync symbol $[A_{N/4}\ -B_{N/4}\ A_{N/4}\ B_{N/4}]$ yields the best performance, followed by the algorithm using Shi's estimator with a degradation of about 2 dB at 10% miss detection probability.

The miss detection probabilities of the coherent ML estimation algorithms using existing and proposed sync signal structures are plotted in Figure 4. As the numerical results show, the joint coherent estimation using our proposed sync signal structure $[A_{N/4}\ -B_{N/4}\ A_{N/4}\ B_{N/4}]$ yields the best synchronization performance, followed by Shi's estimator with a degradation of about 1 dB at 10% miss detection probability.

We further compare the miss detection probabilities of non-coherent and joint coherent ML estimations in Figures 3 and 4 It is not surprising that non-coherent ML estimation has about 8 dB performance degradation compared to joint coherent ML estimation at 10% miss detection probability. This is because the timing detection metric of non-coherent ML estimation has noise correlation term. Therefore, it is sensitive to noise and has poor localizability.

VI. Conclusion

In this paper, we have discussed time and frequency synchronization issues in wireless communication systems. A synchronization signal structure we proposed in an earlier work is extended further. We propose a joint coherent ML estimation algorithm to take advantage of the synchronization signal structure. Performance of the proposed joint coherent ML estimation is simulated and compared to other estimators. It is observed that our proposed method yields better time and frequency acquisition performance than other methods.

References

[1] J. L. Massey, “Optimum frame synchronization,” IEEE Trans. Commun., vol. 20, no. 2, pp. 115-119, Apr. 1972.

[2] G. L. Lui and H. H. Tan, “Frame synchronization for Gaussian channels,” IEEE Trans. Commun., vol. 35, no. 8, pp. 818-829, Aug. 1987.

[3] T. M. Schmidl and D. C. Cox, “Robust frequency and timing synchronization for OFDM,” IEEE Trans. Commun., vol. 45, pp. 1613-1621, Dec. 1997.

[4] H. Minn et al., “A robust timing and frequency synchronization for OFDM systems,” IEEE Trans. Wireless Commun., vol. 2, no. 4, pp. 822-839, July 2003.

[5] K. Shi and E. Serpedin, “Coarse frame and carrier synchronization of OFDM Systems: a new metric and comparison,” IEEE Trans. Wireless Commun., vol. 3, no. 4, pp. 1271–1284, July 2004.

[6] B. Park et al., "A novel timing estimation method for OFDM systems," IEEE Commun. Letters, vol. 7, no. 5, pp. 239-241, May. 2003.
[7] A. J. Coulson, "Maximum likelihood synchronization for OFDM using a pilot symbol: Algorithms," IEEE J. Select. Areas Commun., vol.19, pp. 2486-2494, Dec 2001.
[8] A. J. Coulson, "Maximum likelihood synchronization for OFDM using a pilot symbol: Analysis," IEEE J. Select. Areas Commun., vol.19, pp. 2495-2503, Dec. 2001. R. L.
[9] M. Guenach et al., "Coded-aided ML joint synchronization and channel estimation for downlink MC-CDMA," IEEE J. Select. Areas Commun., vol.24, no. 6, pp. 2486-2494, Jun 2006.
[10] Frank and S. A. Zadoff, "Phase shift pulse codes with good periodic correlation properties," IRE Transactions on Information Theory, vol. 8, no. 6, pp. 381–382, Oct. 1962.
[11] Y. Tsai, G. Zhang, "Time and frequency synchronization for 3GPP long term evolution systems," to appear in IEEE VTC Spring 2007.
[12] 3rd Generation Partnership Project, Technical Specification Group Radio Access Network, Physical Layer Aspects for Evolved UTRA (Release 7), 3GPP TR25.814 V1.0.1 (2005-11).

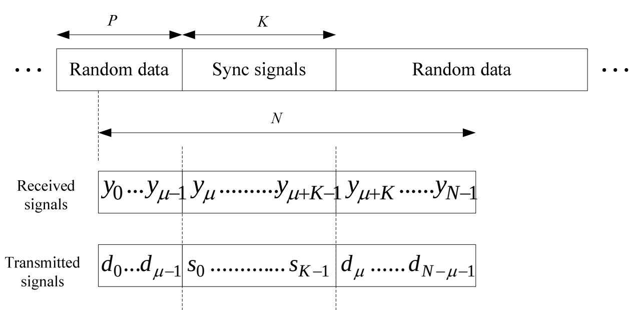

Figure 1: Transmitted and corresponding received data in the synchronization window.

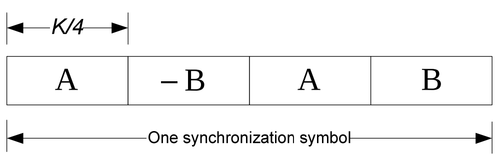

Figure 2: Proposed synchronization signal structure.

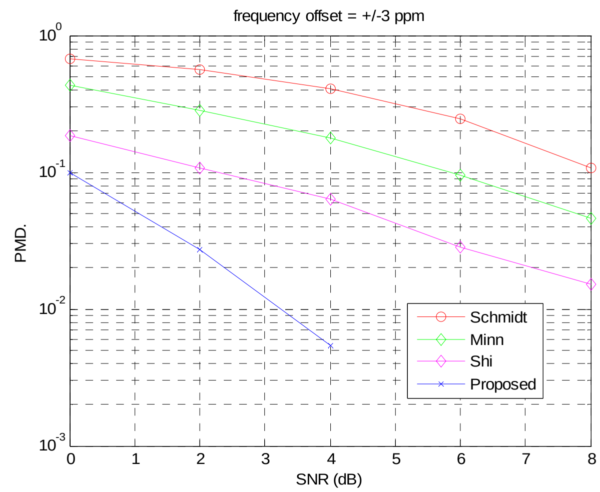

Figure 3: Miss detection probabilities of non-coherent ML estimations.

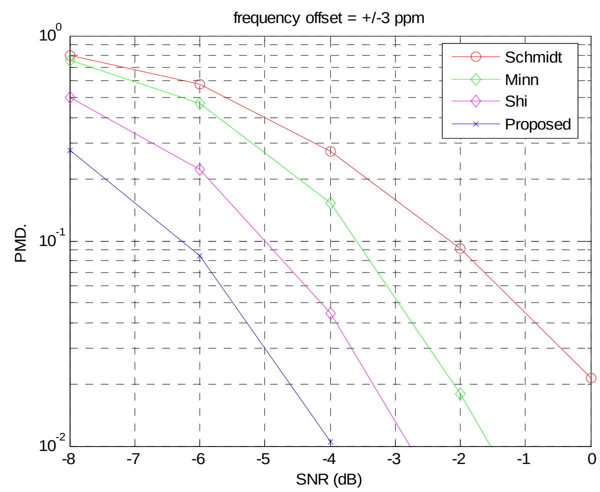

Figure 4: Miss detection probabilities of joint coherent ML estimations.